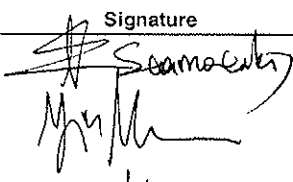
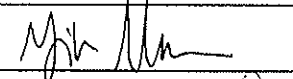
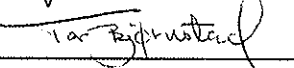


Address	KJELLER NO-2027 Kjeller, Norway	HALDEN NO-1751 Halden, Norway	
Telephone	+47 63 80 60 00	+47 69 21 22 00	
Telefax	+47 63 81 11 68	+47 69 21 22 01	
Report number	IFE/KR/E-2005/002		Date 2005-01-25
Report title and subtitle	Real-time monitoring of calcium carbonate precipitation from geothermal brines		Number of pages 23
Project/Contract no. and name	E-4804 EGS Pilot Plant		ISSN 0333-2039
Client/Sponsor Organisation and reference	EC, SES6-CT-2003-502706		ISBN 82-7017-502-1
Abstract	<p>The objective of the present work has been to study calcite scale formation in geothermal wells. Effective scale management requires on-line monitoring of scaling tendencies as well as detection and identification of scale deposits. In that respect, a gamma-ray attenuation technique was designed and evaluated in the lab for the real-time measurements of scale formation under flow conditions. As a first step we have obtained a preliminary thermodynamic prediction of the stability of a specific geothermal brine (GPK2-S2), regarding CaCO_3 precipitation, under various P-T conditions, using the MultiScale simulation tool. Based on the tool's outcomes the experimental work for the study of calcite scale formation focused on confirming the results. The aim was to find the lowest system pressure at which no scale takes place under specific conditions (temperature, water composition, inhibitor concentration). The precipitation rates for calcite scale in absence and presence of a scale inhibitor were also obtained in the course of this study.</p>		Distribution E. Stamatakis C. Chatzichristos J. Muller E. Brendsdal J. Sagen O. Huseby A. Haugan M. Seiersten T. Bjørnstad Library File
Keywords:			
	Name	Date	Signature
Author(s)	E. Stamatakis J. Muller C. Chatzichristos	2005-01-24	
Reviewed by	J. Muller	2005-01-24	
Approved by	T. Bjørnstad	2005-01-25	

Contents

1	Introduction	1
2	The Soultz-sous-Forêts case history	1
3	Real-time scale detection methods	3
4	General theory	4
5	Experimental design	5
6	Results and discussion	7
6.1	Preliminary data simulation	7
6.2	Experimental results.....	10
6.3	Scale thickness calculations	14
6.4	Mass balances	17
7	Conclusions	18
8	References	19
8.1	<i>Web site references</i>	20

Appendix 1 – Result file from a single point calculation at 1 bar, 160°C

1 Introduction

The production, utilization and/or reinfection of brine found in geothermal reservoirs is often hampered by serious and very unique scale problems. Some of these scale problems are so severe that entire field operations are endangered. The scale deposits encountered in geothermal operations basically follow trends similar to those found in oil fields. However, there are some major differences between the oilfield and geothermal scale formations that are caused mainly by the following parameters, which are encountered in the geothermal fields:

- high temperatures (up to 350°C) and generally low pressures,
- huge mass flow rates,
- “exotic” reservoirs.

The term “exotic” is concerned with the chemical type of reservoirs from which the different geothermal brines are produced. Either the brine or the reservoir rock show chemical compositions not normally found in oilfield reservoirs that can lead to “unusual” types and magnitudes of scale deposits. The huge flow rates of geothermal wells also cause major problems in regard to the formation of scale. Even if only a few milligrams of scale per liter brine would be deposited, large accumulations could be formed due to the large mass flow rates. In addition, the hydrodynamics themselves may play a major role in the formation of scale. However, only few studies can be found that take into account the effect of the flow velocity on the precipitation process (Stamatakis et al., 2005b).

Finally, high temperatures and large temperature drops during geothermal operations promote the deposition of “heat sensitive” compounds, e.g. compounds showing a marked decrease of the solubility with decreasing temperature, such as BaSO_4 , SiO_2 , heavy metal sulfides, etc. The “pressure sensitive” scales (e.g. CaSO_4) are normally less of a problem with the exception of CaCO_3 . In the case of CaCO_3 , the solubility of the compound does not play the major role; instead, pressure drops lead to a chemical change of the dissolved species (CO_2 flashing), resulting to chemical reactions, which increase the product of the concentrations of the precipitating ions (Ca^{2+} , CO_3^{2-}) above the solubility product, which – in turn – leads to precipitation. A serious problem occurs when carbonate scales precipitate from produced fluids containing acid gases.

Reduction in pressure during production outgasses the fluid, which raises pH and causes scale deposition. The deposition of carbonate can extend from the near-wellbore matrix, along tubing and into surface equipment as the produced water continuously changes in pressure and temperature. The pressure drop at the point of entry into the wellbore can lead to matrix scale. Subsequent release of pressure from the wellhead to surface can lead to massive deposits of scale in surface equipment and tubing (Crabtree et al., 1999).

2 The Soultz-sous-Forêts case history

The Soultz-sous-Forêts geothermal field is on the Alsace region in northeast France. The field is a Hot Dry Rock (HDR) reservoir and its location is shown in figure 1. The

reservoir extends along NNW/SSE, about 500 m wide, 1500 m long and 1500 m tall. The HDR concept itself is very simple but the development of the associated technology has taken significantly longer than anticipated. This concept consists briefly of:

- use the natural fracture systems in the basement rocks,
- enlarge its permeability through massive stimulation,
- install a multi-well system,
- through pumping and lifting, force the water to migrate through the fracture system of enhanced permeability ("reservoir") and use the heat for power production,
- use submersible pumps to increase fluid recovery.

A report uses 4 levels of headings. If you need more, use ordinary fonts and make it bold. Level one has size 14 and bold. The others are 12 and bold.

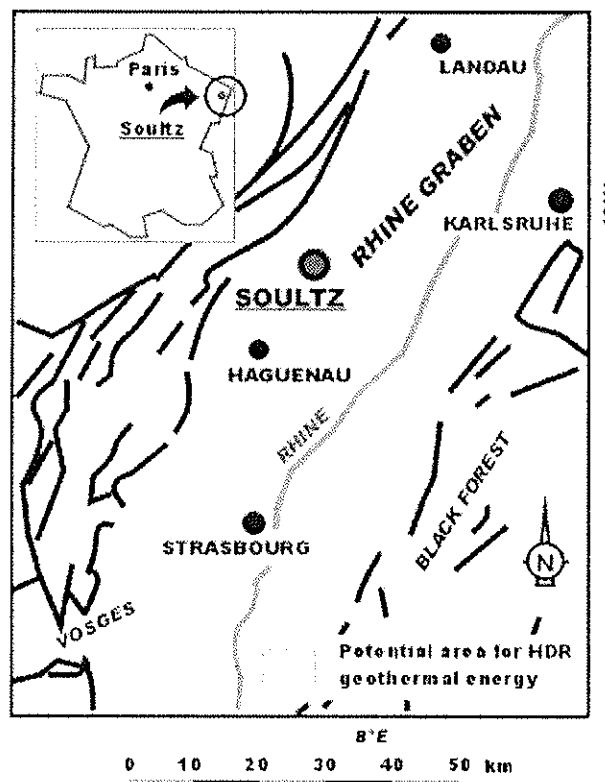


Figure 1 – The European HDR-project is situated in Soutz-sous-Forêts, France, at the western border of the Rhine Graben.

The fracture network at Soutz-sous-Forêts has been explored down to 5000 m depth. The predicted temperature of 200° C was measured at a depth of 4950 m. Within the volume, which has been investigated the network appears to be stable and to have the desired properties. GPK2 is planned as a production well for the Scientific Pilot Plant. The final planned Scientific Pilot Plant module is a 3-well system consisting of one injector and two producers, one on each side of the injector. All wells are started from a single platform using the existing deep well GPK2 as one of the producers. By 2006,

this facility should be capable of producing around 6 MW of electricity (for more details about Soultz-sous-Forêts project visit the web site: www.soultz.net).

A hydraulic stimulation was led in July 2000 for GPK2 well, one year after deepening it up to 5000 m. The geochemical results obtained during the monitoring of the fluid produced from this well have been provided to our research group in order to study calcite scaling tendency. Table 1 contains the water analysis for the geothermal brine, which has been used for this study. The overall objective of this study is the scaling management optimization (optimize the surface processes in order to minimize the impact of calcite scaling). It is understood that the only parameter available for optimization is the pressure, which currently is held at 20 bars in order to avoid scaling. In addition, the use of inhibitors to prevent scaling is examined since its potential successful application will permit large reduction in required pressure.

Table 1 – Water analysis for geothermal brine GPK2 –S2.

Ion	Concentration	
	mmol/l	mg/l
Na ⁺	1225.47	28173.56
K ⁺	73.66	2880.11
Mg ²⁺	3.09	75.12
Ca ²⁺	165.92	6650.07
Fe ²⁺	1.74	97.18
Cl ⁻	1630.47	57800.16
SO ₄ ²⁻	1.78	170.99
Total alkalinity	6.60	402.72
Fixed gas composition		
CO ₂	14.20 mole%	
H ₂ S	0.00 mole%	

Effective scale management requires on-line monitoring of scaling tendencies as well as detection and identification of scale deposits. In that respect, a gamma-ray attenuation technique was designed and evaluated in the lab for the real-time measurements of scale formation under flow conditions. The precipitation rates for calcite scale in absence and presence of a scale inhibitor were also obtained in the course of this study.

3 Real-time scale detection methods

Laboratory determinations of real-time scale deposition were recently reported using a radiotracer technique (Stamatakis et al., 2005a), an attenuated total reflection sensor (Smith et al., 2003), a rotating disk electrode technique (Morizot & Neville, 2000), tapered optical fibers (Moar et al., 1999), a piezoelectric sensor (Emmons et al., 1999) and an ultrasonic technique (Gunarathne & Keatch, 1995). In addition, various nuclear attenuation techniques for the *in-situ* detection of mineral scale in actual production systems have been also reported recently. In particular, a handled device was developed to detect the presence of scale in surface piping by measuring the nuclear attenuation across the pipe diameter and two field cases were presented in which a dual-energy-venturi multiphase flow meter was used to detect and characterize scale according to the attenuation of the nuclear spectrum (Theuveny et al., 2001). A year later, Poyet and co-researchers presented a gamma-ray attenuation method, based on continuous triple-energy gamma-ray attenuation measurements, for the detection of scale deposition in real-time in oilfield production tubulars (Poyet et al., 2002). The last method was actually an extension of previous work that had been applied to several field cases of surface pipe scale detected by dual-energy attenuation measurements (Kevin, 1999).

The method enables a simple monitoring device to detect and characterize scale in its earliest stages of formation.

4 General theory

The attenuation of gamma radiations through composite materials is of wide interest for industrial, medical and agricultural studies. There is an important parameter for characterizing the penetration and diffusion of gamma rays in the medium, which is called attenuation coefficient. The percentage of γ -ray energy absorbed by the material is due to a process known as electron ionisation; this is dependent upon the material density and atomic number. As a result the detected γ -ray attenuation provides a picture of the absorbed energy on the irradiated objects.

The absorption of the γ -ray radiation by a material is proportional to the degree of γ -ray attenuation and is dependent on the energy of the γ -ray radiation and the following material parameters:

- thickness;
- density;
- atomic number;

The relationship between these values can be described by:

$$I_x / I_0 = \exp[-(\mu / \rho)\chi] \quad (1)$$

where, I_x is the intensity of the γ -ray radiation after passing through a material, I_0 is the intensity of the narrow beam monoenergetic γ -ray radiation before passing through a material, μ is the linear attenuation coefficient, ρ is the material density, and x is the mass thickness. Note that the mass thickness is defined as the mass per unit area, and is obtained by multiplying the thickness t by the density ρ , i.e., $x = \rho t$.

An important component in eq.1 is the mass attenuation coefficient $\mu_m = \mu/\rho$. The mass attenuation coefficient represents the penetration and the energy deposition by the photons in materials. This can be obtained by the measurement of I_0 and combination with the confirmed values of I_x and x . Research has involved in obtaining this value for radiological interest, as this value is characteristic for each element, mixture and compound.

Equation (1) can be rewritten as

$$\chi = (\mu / \rho)^{-1} \ln(I_0 / I_x) \quad (2)$$

from which the mass thickness χ can be obtained from measured values of I_0 and I_x .

Instead of expressing gamma-rays absorption in terms of attenuation coefficients it is sometimes more explicitly stated in units of half-value layers (or thickness) of the particular absorber. One half-value thickness is the quantity of material, either in grams per square centimeter or in centimeters, required to reduce the intensity of gamma rays of a particular energy to one-half its initial value at the surface. The half-value thickness, $d_{1/2}$ is related to the linear attenuation coefficient μ by $d_{1/2} = 0.693/\mu$.

5 Experimental design

Figure 2 shows the schematic diagram of the experimental apparatus, which was designed and constructed for this study. Twin HPLC pumps drive two solutions, one containing scale forming cations (Ca^{2+}) and the other anions (HCO_3^-). The solutions are pumped through two pre-heating tubes, which raise the solution temperature to the desired test temperature prior to arriving at the mixing point. The combined solution, which now has a positive saturation index, passes through our test session (1m long aluminium 6061 with 1cm ID) and scale crystals nucleate and grow on its internal surface. The temperature is maintained constant by a heating equipment fixed along the tube.

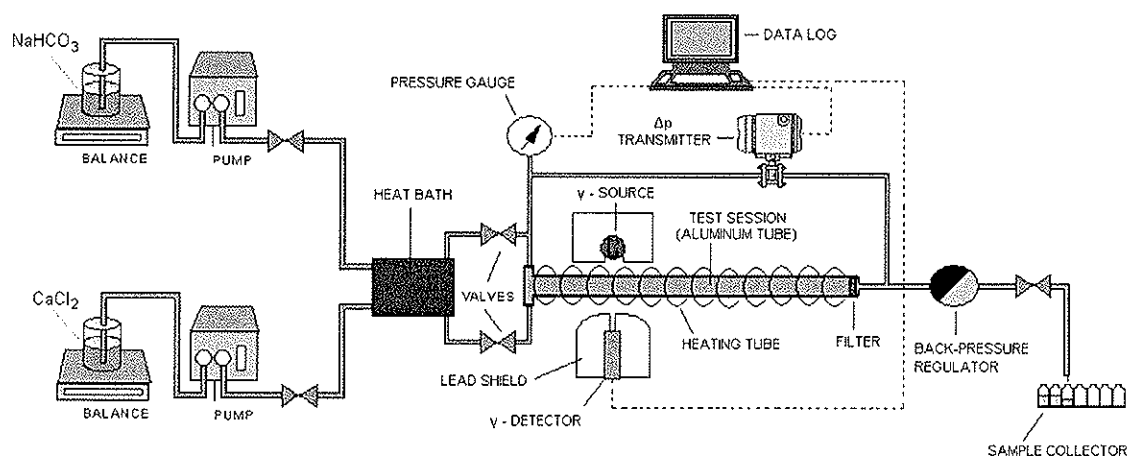


Figure 2 – Experimental set-up illustration.

To monitor the forming scale, a narrow beam of gamma rays from an appropriately shielded radioactive source (^{131}Ba) is directed through the tube; variations in the transmitted intensity recorded by a radiation detector positioned on the opposite side of the tube can then be related to the variations in the mass per unit area of the intervening deposited material (see figure 3). In a narrow beam conditions the attenuation of the measured radiation follows a strictly exponential relationship with the thickness of the absorber expressed as in eq.(1). If we consider a single energy of the source emission, calculations of the attenuation of γ -ray beams are thus easy if also the attenuation coefficients of the materials are known. For that reason, the energy window of the radiation detector was chosen from 360 keV and upwards so as a single energy measurement at approximately 500 keV could safely be assumed (note that when ^{131}Ba disintegrates to ^{131}Cs , gamma radiation with energies of 496 keV, 373 keV, 216 keV and 124 keV is emitted).

To obtain the final profile of the deposits, the tube was moved across the mounted source and detector, and measurements were collected at certain intervals at the end of each run.

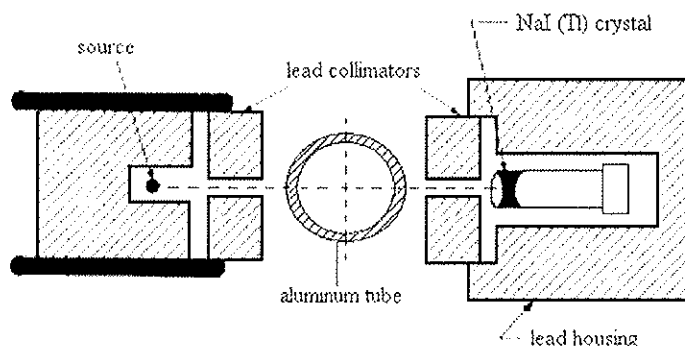


Figure 3 – Schematic γ -ray narrow beam adsorption measurement.

To keep the experimental work as simple as possible, no gas phase is present in the system. For that reason, the two scaling solutions have been modified in that way so as after mixing them at 1:1 ratio we get a similar scaling tendency as that of the desired geothermal brine (see Table 1). Table 2 shows the water analysis of the modified brine 1, which was prepared for this study. Brine 1 exhibits similar scaling tendency, regarding calcite formation, to the geothermal brine GPK2 –S2. Different concentrations of a standard phosphonate type scale inhibitor (Amino Methylene Phosphonic acid Disodium Salt, Na_2AMP) were added into the scaling solutions in order to study its performance. This inhibitor product has been provided by MI-Production Chemicals and it is suitable for carbonate scales.

Table 2 – Water analysis for modified brine 1 after mixing solutions 1 & 2 in a 1:1 ratio.

		Concentration	
		mmol/l	mg/l
solution 1	CaCl_2	330	36624.5
	NaCl	1200	70130.9
solution 2	Na HCO_3	14	1176.1
	NaCl	1200	70130.9

The choice of aluminum 6061 as the test session in our experimental system was based mainly for two reasons; its low density (2.70 g/cm^3) compare to other materials such as steel and iron, and its acceptable behavior to corrosion especially in absence of H_2S (Burda et al., 1983). Generally the lower the density the more transparent the material is to the γ -rays and, therefore, the higher the accuracy for the measurements of the scale thickness with the implemented technique.

6 Results and discussion

6.1 Preliminary data simulation

The computer model multiSCALE v.5.1 performed the preliminary thermodynamic predictions of the stability of the geothermal brine provided to this study. MultiScale is commercialized by Petrotech ASA, and is considered internationally to be the state of the art when it comes to CaCO_3 scale prediction. MultiSCALE contains an accurate model for aqueous equilibria and a complete PVT-model. This makes it a suitable tool to predict scaling of calcium carbonate. Precipitation of carbonates involves calculation of pH and the 3-phase distribution of water, organic components and acids. In addition to predict carbonate formation based on equilibrium thermodynamics, the kinetics of the scale forming reactions is also considered.

Using the water analysis provided from Table 1, various profile curves were produced by multiSCALE. The result file from a single point calculation at 1 bar, 160°C using the multiSCALE's fixed gas composition model with 14.2 mole% CO_2 is given in Appendix A. Single point calculations give the most comprehensive result file including a list over the numerical errors in the calculations. The results in Appendix A are at equilibrium including precipitation. From this file one can note that at these conditions (1 bar, 160°C) there is a significant amount of CaCO_3 , which precipitates (160.1 g/m³). The calculated initial saturation ratio, SR, is 20.016. Moreover, although the Fe^{2+} content of the geothermal brine is quite low (1.74 mmol/l) compared with the Ca^{2+} content (165.92 mmol/l) there is a large amount of FeCO_3 that also precipitates (115 g/m³). Running a new calculation by tuning the Fe^{2+} content of the brine to zero, the precipitated amount of CaCO_3 is almost doubled, even though this tuning does not influence its initial SR (see Table 3 below).

Table 3 – Saturation ratios and precipitated masses for $\text{Fe}^{2+} = 0$ mmol/l.

Salt	Initial SR	Precipitate g/m ³	Equilibrium SR	Solubility product
FeCO_3	0.000	0.0	0.000	4.2902E-10
CaCO_3	20.017	259.7	1.000	9.3646E-08
NaCl	0.022	0.0	0.022	9.1414E+01

After running the single point calculation type at constant temperature and pressure we then performed few pressure and temperature profiles of the geothermal brine GPK2 – S2. These profiles are just automatically generated series of single point calculations and they are very helpful for the thermodynamic prediction of the stability of the corresponding geothermal brine at various P, T. Two temperature profiles from 0 to

200°C at constant pressures of 1 bar and 20 bars respectively (figures 4, 5), and another two pressure profiles from 1 bar to 25 bars at constant temperatures of 160 and 185°C (figures 6, 7) are illustrated bellow.

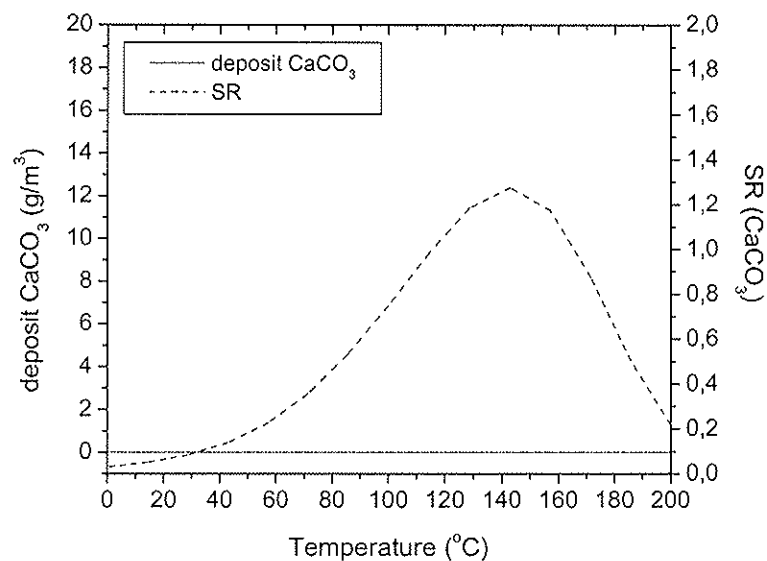


Figure 4 – Temperature profile for geothermal brine GPK2 –S2 at 20 bars.

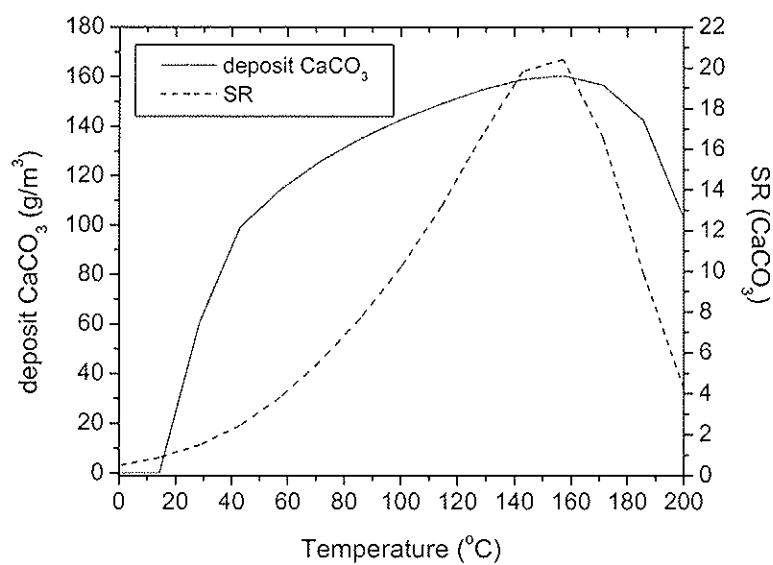


Figure 5 – Temperature profile for geothermal brine GPK2 –S2 at 1 bar.

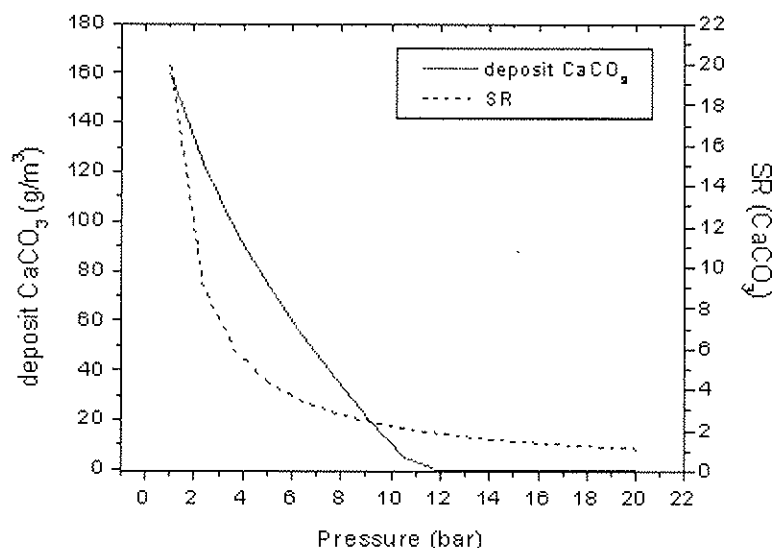


Figure 6 – Pressure profile for geothermal brine GPK2 –S2 at 160°C.

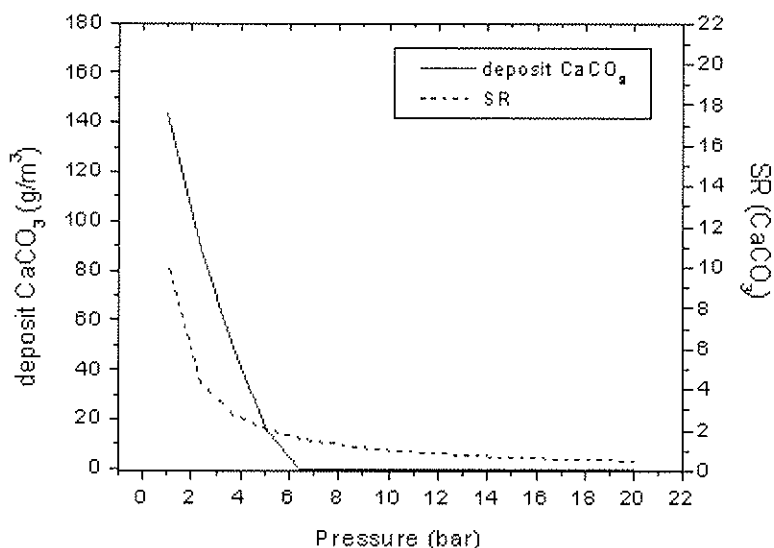


Figure 7 – Pressure profile for geothermal brine GPK2 –S2 at 185°C.

The results from these profiles can be summarized as follow:

No CaCO₃ precipitation at 20 bars system pressure regardless the temperature.

Precipitated CaCO₃ reaches a maximum at brine temperature of 140 – 160 °C at 1 bar.

At 160°C the pressure has to be greater than 11 bars to avoid CaCO₃ precipitation while at 185°C it has to be greater than only 6 bars.

Based on the above profile curves the experimental work for the study of calcite scale formation focused on confirming/correcting/extending these profiles. The aim was to find the lowest system pressure at which no scale takes place under specific conditions (temperature, water composition). A phosphonate type scale inhibitor (Na₂AMP) was finally used in order to check if and how much the pressure could further be reduced.

6.2 Experimental results

Table 4 contains a list with all the laboratory experiments performed.

Table 4 – List of the laboratory experiments.

RUN	Brine	T (°C)	P (bar)	Q (ml/min)	t_{ind} (min)	Na ₂ AMP (ppm)
1	1	160	15	1	∞	-
2	1	185	15	1	∞	-
3	1	185	10	1	<1	-
4	1	185	10	1	∞	100
5	1	185	10	1	~60	10
6	1	185	10	1	~10	1
7	2	185	10	1	<1	-

∞ denotes no scale

In Table 4, brine 1 corresponds to the modified brine as defined in Table 2. In run 7 another brine (brine 2) was used. Brine 2 is quite similar to brine 1, but also contains all the ions at the same concentrations as the real geothermal brine GPK2 –S2, and its water analysis is demonstrated in Table 5. The reason for using brine 2 in our experimental investigation was to check if and how these ions (Mg^{2+} , Fe^{2+} , K^+) can influence calcite precipitation.

Table 5 – Water analysis for modified brine 2 after mixing solutions 1 & 2 in a 1:1 ratio.

		Concentration	
		mmol/l	mg/l
solution 1	CaCl ₂	330	36624.5
	NaCl	1200	70130.9
	MgCl ₂	6	571.2
	KCl	75	5591.3
solution 2	NaHCO ₃	14	1176.1
	FeSO ₄	4	607.6
	NaCl	1200	70130.9
	KCl	75	5591.3

From Table 4 one may note that there was no calcite scale formation at 15 bars both at 160 and 185°C and this is in agreement with the multiScale simulation results. However, scaling took place at 185°C and 10 bars, when multiScale suggests that at 185°C there would be no scale when the pressure is above 6.1 bars (see figure 8). No scale was also observed at 185°C and 10 bars when 100 ppm of the scale inhibitor Na₂AMP were added into brine 1. Figure 8 illustrates the gamma attenuation measurements for the experimental runs 3-6, where the influence of the added scale inhibitor on calcite formation is recorded. The measurements were obtained using the γ -ray narrow beam adsorption system (see figure 3), 10 cm from the inlet of our test session.

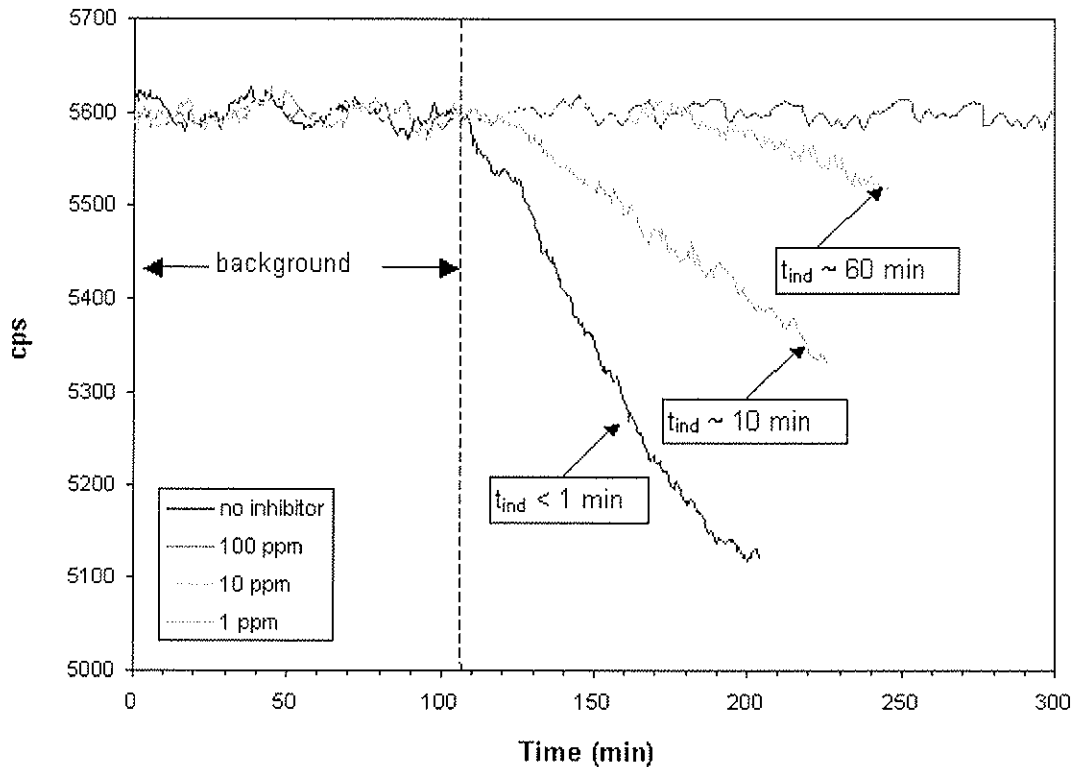


Figure 8 – Gamma attenuation measurements for calcite precipitation in the presence and absence of the inhibitor Na_2AMP at a fixed position of the tube (10cm from inlet) at 185°C (runs 3-6).

In order to measure the background gamma attenuation in figure 8, we started pumping through the aluminum tube only the CaCl_2 solution. Then, exactly after 109 min we started pumping the NaHCO_3 solution too. The *experimental* induction time, t_{ind} , of precipitation is defined as the time which elapses between the creation of supersaturation and the first observable change in some physical property of the precipitating (scaling) system, e.g. the appearance of crystals, change in solution conductivity, composition, pH, a change in pressure drop etc (Söhnel and Mullin, 1982). An experimentally measured induction period is therefore dependent to some extent on the method of detection. Particularly for the gamma-attenuated method, we define the induction time as the time, which elapses between the first addition of NaHCO_3 solution into our test session, and the time when the counting rate R significantly reduces. Of course, we have to mention that the source/detector system is not placed at the inlet of the tube but 10 cm away of it and the present implemented method is not measuring the “real” induction time.

In figure 9, the gamma-attenuated distribution of the deposits is illustrated for the same runs. The red line corresponds to the background attenuation measurement, e.g. the measurement taken when the aluminum tube was filled only with solution 1 of brine1. It is important to mention here that solution 1 and the mixed brine 1 have identical densities defined from NaCl concentration. This point is crucial since the attenuation technique can detect small changes in the fluid density. It is seen from figure 9 that introduction of inhibitor distributes scale homogeneously across the tube, contrary to the case with no inhibitor. In the later case no scale is monitored after 35-40 cm.

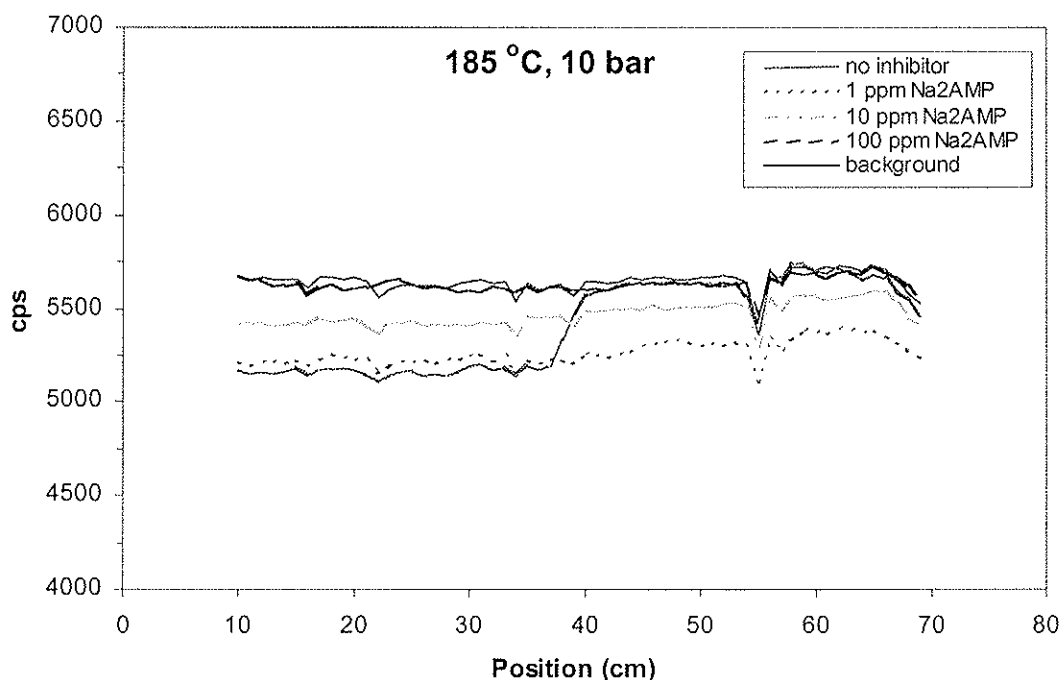


Figure 9 – Gamma-attenuated distribution measurements across the tube in the presence and absence of the inhibitor Na_2AMP at the end of each run.

Figure 10 shows the differential pressure buildup across our test session in the presence and absence of the scale inhibitor. It is obvious from figures 8 and 10 that the attenuation technique gives a much faster response for the onset of calcite precipitation compare to the Δp monitoring.

To check the actual behavior of the geothermal brine GPK2 –S2, brine 2 (see Table 5) was also prepared at the lab and used for this study. Figure 11 compares the gamma-attenuated distribution of brine 1 and 2 together with the background measurement (red line). It is clear from that figure that the two brines exhibit more or less similar scaling distribution tendency. In particular, both brines gave significant calcite deposition in the first 35-40 cm of the tube and almost nothing further in. In figure 12 we compare the Δp buildups from those two brines.

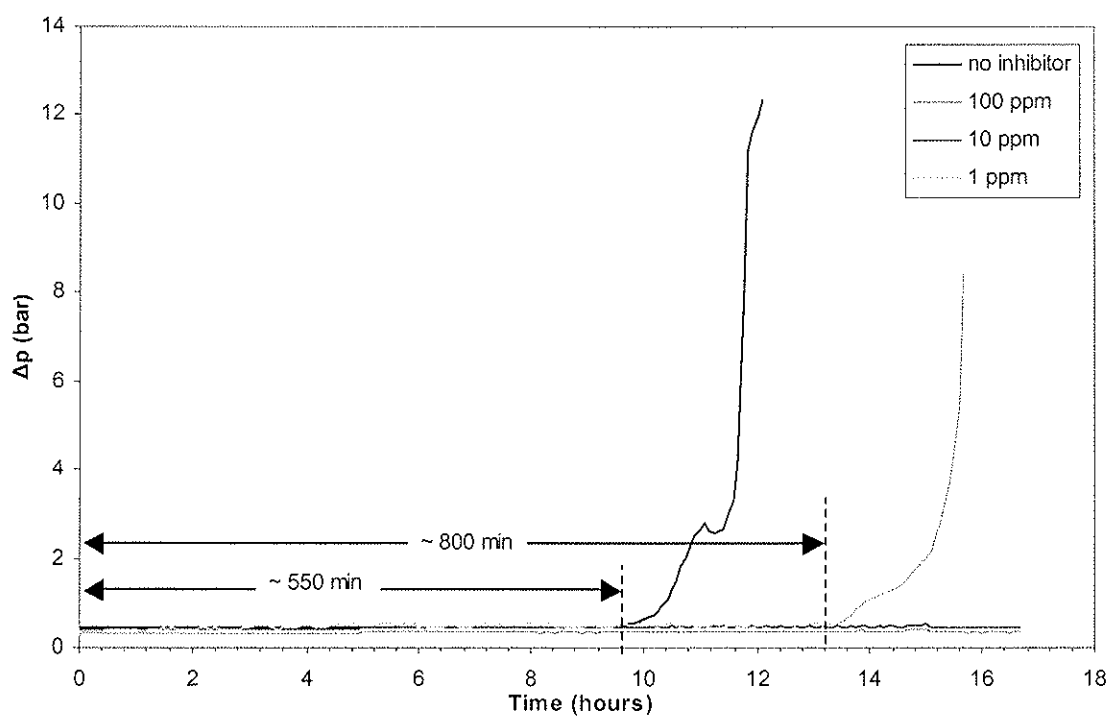


Figure 10 – Δp buildup in the presence and absence of the inhibitor Na_2AMP at 185°C , 10 bars (runs 3-6).

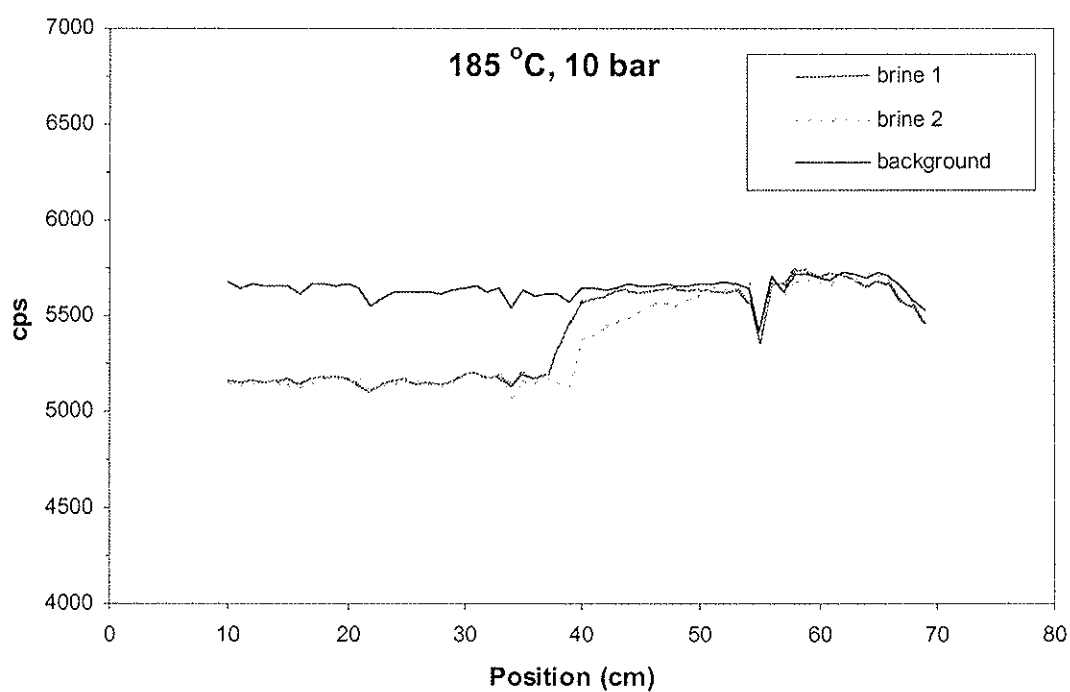


Figure 11 – Gamma-attenuated distribution measurements across the tube for the two modified brines at 185°C , 10 bars (runs 3, 7) at the end of each run.

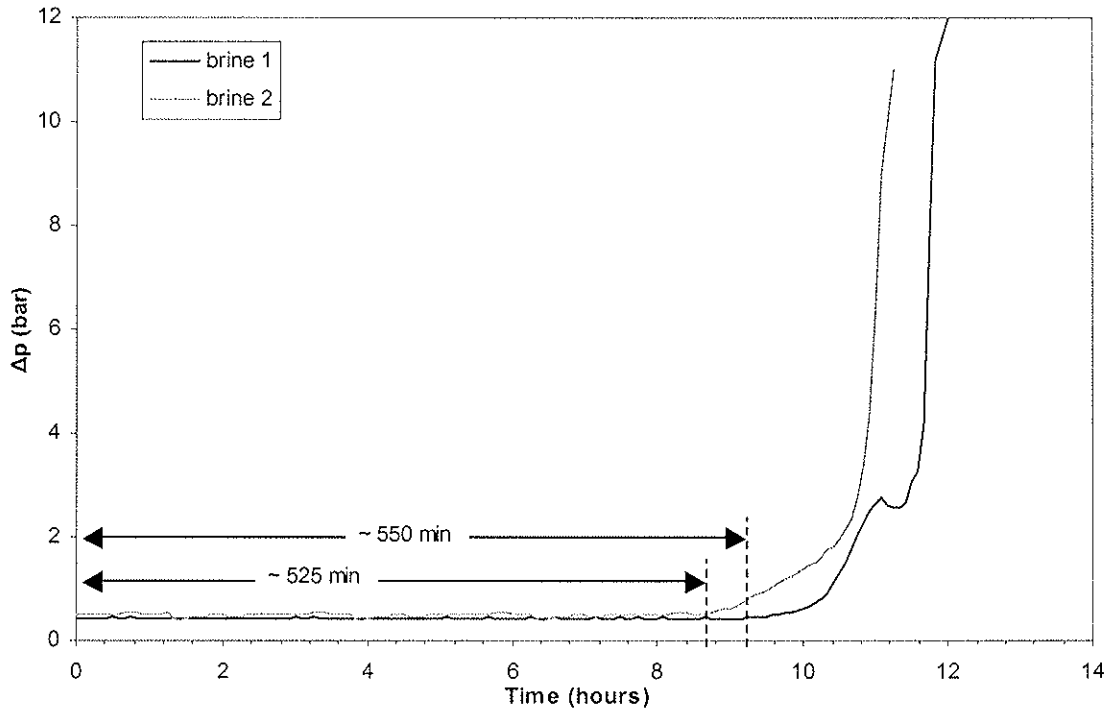


Figure 12 – Δp buildup along the tube for the two modified brines.

6.3 Scale thickness calculations

Equation 1 gives the decrease of the gamma rays intensity for a homogeneous absorber. If the beam of gamma rays enters a different dense medium eq.1 has to be modified. It can be easily shown that when a narrow beams of gamma rays passes through our test session (aluminum tube) to the forming calcite scale, and finally, to the water phase, the gamma ray intensity decreases as:

$$I / I_0 = e^{-(\mu_s - \mu_w)t} \quad (3)$$

where, I is the intensity of the γ -ray radiation after passing through the scaling system, I_0 is the intensity of the γ -ray radiation after passing through the aluminum tube filled only with water (no scale), μ_s is the linear attenuation coefficient for solid CaCO_3 , μ_w is the linear attenuation coefficient for water, and t is the thickness of the scale.

From existing tables (Shleien, 1992), the linear attenuation coefficients for solid CaCO_3 and water were calculated at 500 keV as:

$$\mu_s = 0.164 \text{ cm}^{-1}, \mu_w = 0.067 \text{ cm}^{-1}$$

Then, the thickness t can easily be obtained from measured values of I_0 and I_x as:

$$t_{(cm)} = \frac{\ln(I_0 / I)}{0.097} \quad (4)$$

For the scale thickness measurements at the fixed position we measure an average I_0 of 5605 counts per seconds (cps). Using eq.(4) the following scale thickness profiles

curves were computed (figure 13). As may be seen from those profiles, the increase of the scale thickness in the presence and absence of the inhibitor Na_2AMP follows a linear curve from the slope of which the calcite scaling rate at a single position (10 cm from the inlet) can be calculated.

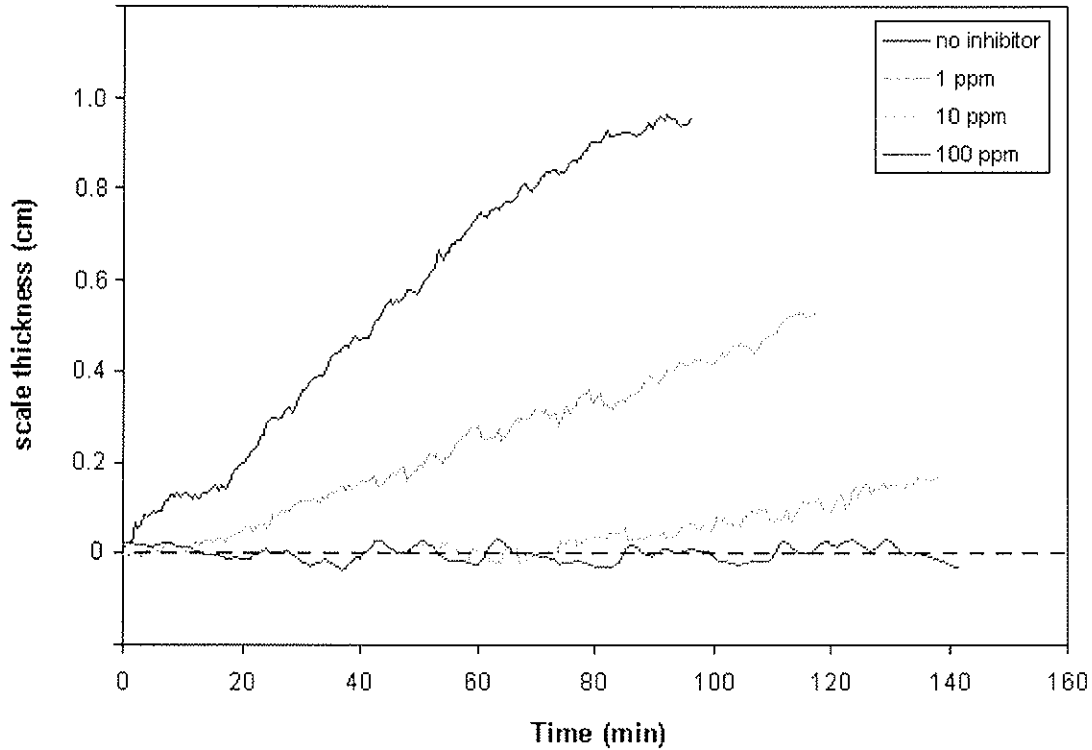


Figure 13 – Scaling rates (scale thickness as a function of time) of calcite precipitation in the presence and absence of the inhibitor Na_2AMP at a fixed position of the tube (10cm from inlet).

From eq.(4), it is easy to calculate the distribution of the scale thickness across the tube. For this case, a distributed I_o was initially measured across the tube (see background curve in figure 9). Figure 14 illustrates the scale thickness distribution inside our test section in the presence and absence of the inhibitor Na_2AMP , while figure 15 shows the scale thickness distribution for the two modified brines 1 and 2 at the end of each run.

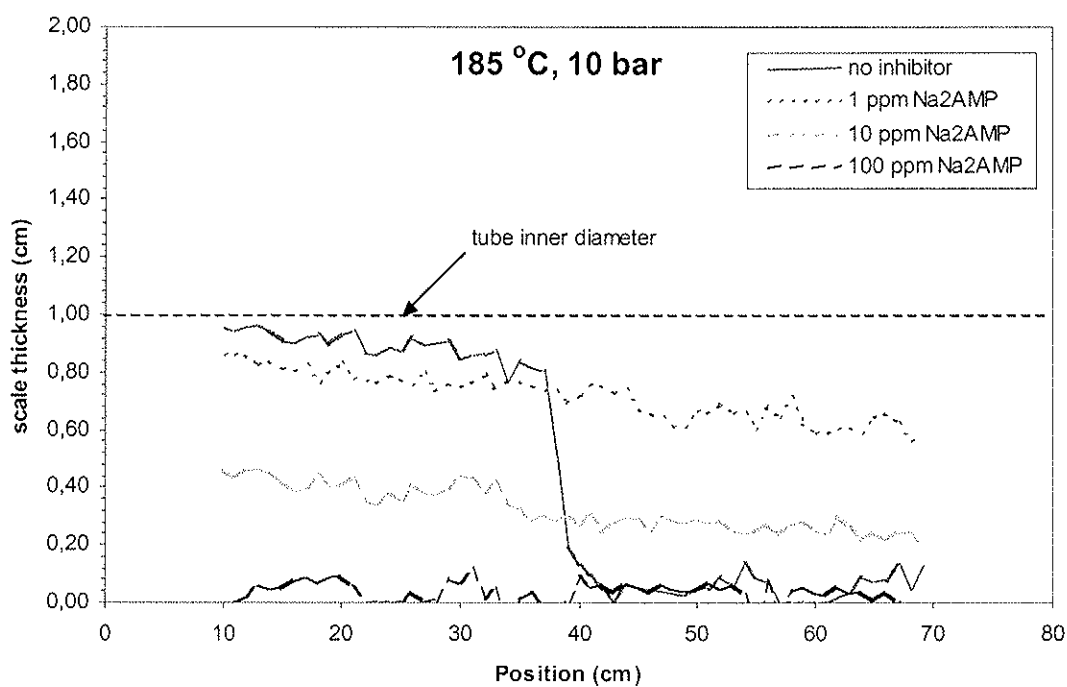


Figure 14 – Scale thickness distribution across the tube in the presence and absence of the inhibitor Na_2AMP at the end of each run (runs 3-6).

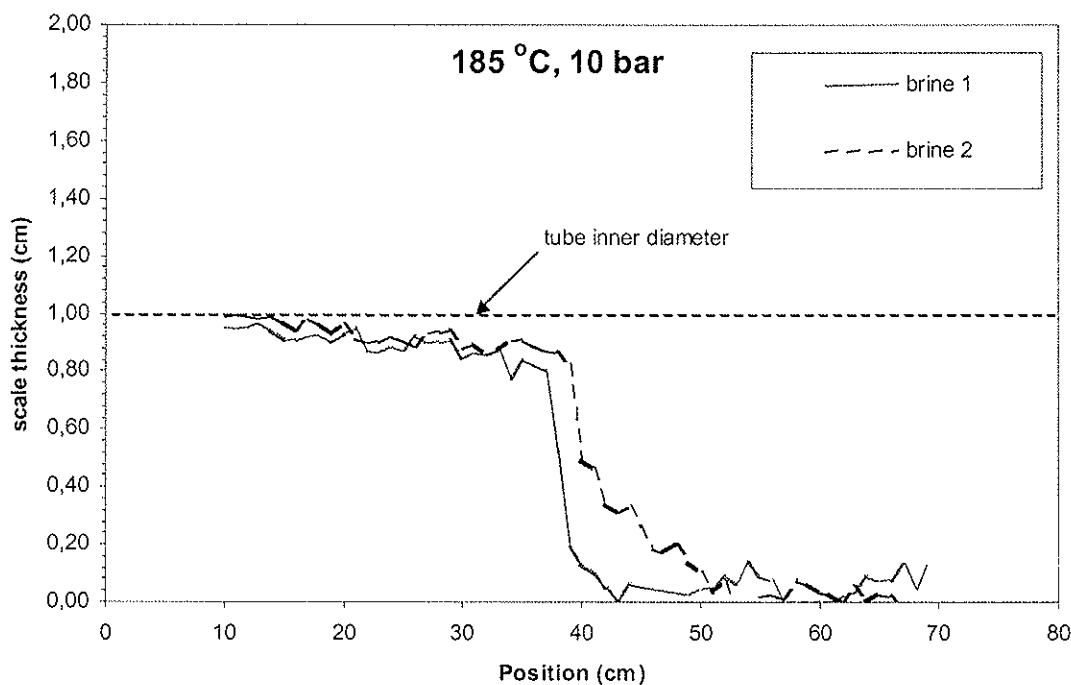


Figure 15 – Scale thickness distribution across the tube for the two modified brines at the end of each run (runs 3, 7).

6.4 Mass balances

Samples were also collected periodically (every 20 min) at the exit end of the scaling tube and analyzed for Ca^{2+} , Mg^{2+} and Fe^{2+} , depending on the initially used brine (1 or 2), using an ICP-MS analyzer. Figure 16 illustrates the Ca^{2+} concentration at the outlet, obtained from the analysis of the samples from all experimental runs (runs 1-7).

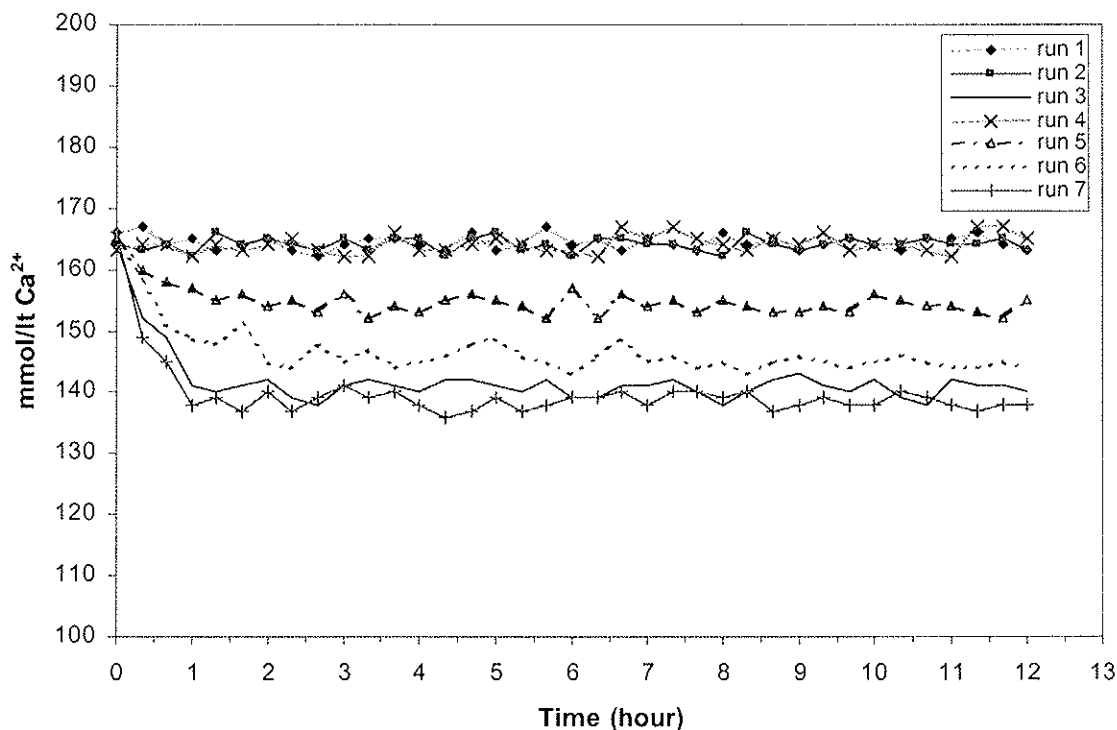


Figure 16 – Ca^{2+} conc. at the outlet for runs 1-7.

When brine 2 was used in our investigation (run 7), analysis of the Mg^{2+} and Fe^{2+} content was also carried out. The analysis showed (see figure 17) that there is no ion loss. This fact suggests that CaCO_3 is the only salt, which precipitates from brine 2. This is contrary to the simulation results from MultiScale. The tool predicts a significant amount of FeCO_3 precipitation when Fe^{2+} ions are present even in a quite low concentration.

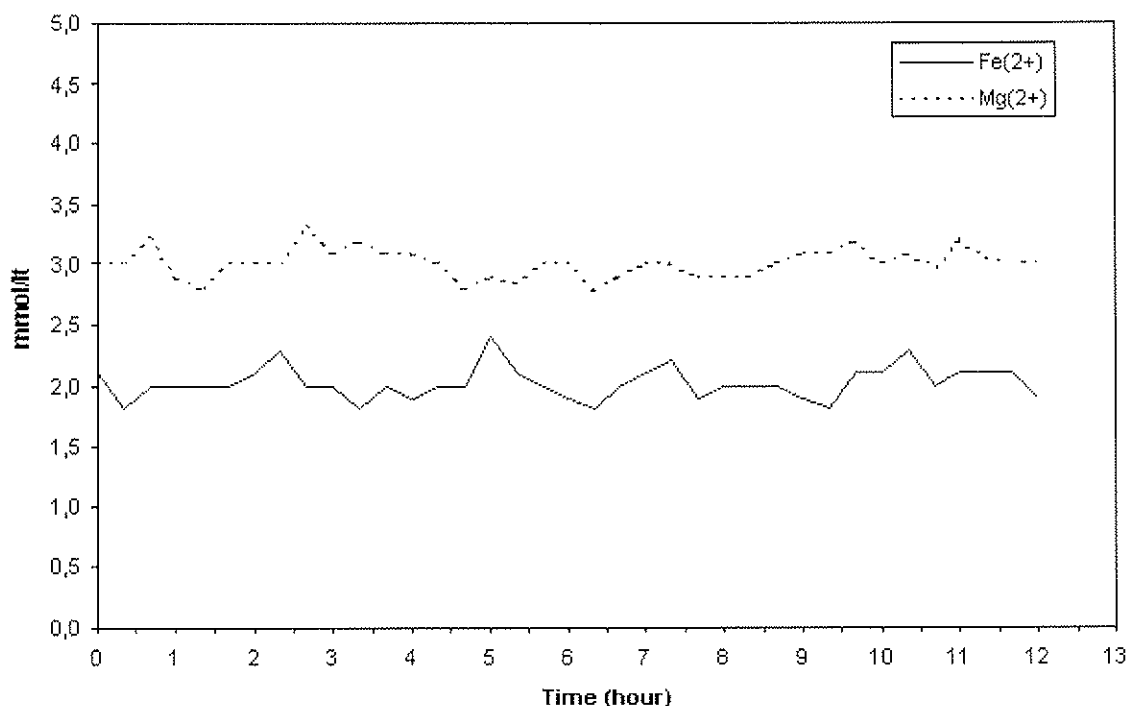


Figure 17 – Mg^{2+} and Fe^{2+} conc. at the outlet for run 7.

7 Conclusions

A gamma-ray attenuation technique was designed and evaluated in the lab for the real-time measurements of scale formation under flow conditions. It was found that the attenuation technique gives a much faster response for the onset of calcite precipitation compare to the Δp monitoring.

As a first step in this study we have obtained a preliminary thermodynamic prediction of the stability of a specific geothermal brine (GPK2-S2), regarding $CaCO_3$ precipitation, under various P-T conditions, using the MultiScale simulation tool. The results from the simulations can be summarized as follow:

No $CaCO_3$ precipitation at 20 bars system pressure regardless the temperature.

Precipitated $CaCO_3$ reaches a maximum at brine temperature of 140 – 160 °C.

At 160°C the pressure has to be greater than 11 bars to avoid $CaCO_3$ precipitation. while at 185°C it has to be greater than only 6 bars.

Based on the MultiScale's outcomes the experimental work for the study of calcite scale formation focused on confirming the results. The aim was to find the lowest system pressure at which no scale takes place under specific conditions (temperature, water composition, inhibitor concentration). The results from the gamma-ray attenuation technique showed that there was no calcite scale formation at 15 bars both at 160 and 185°C and this is in agreement with the multiScale simulation results. However, scaling took place at 185°C and 10 bars, when multiScale suggests that at 185°C there would be

no scale when the pressure is above 6.1 bars. No scale was also observed at 185°C and 10 bars when 100 ppm of the scale inhibitor Na₂AMP were added into brine 1. This fact suggests that system pressure can further be reduced with the addition of an appropriate scale inhibitor. The presence of inhibitor distributes the scale more homogeneously across the tube, contrary to the no inhibitor case where no scale is monitored after 35-40 cm.

8 References

- Burda P. A., Chhatre R. M., Nekoksa G., Hanck J. A., "Materials corrosion during the secondary H₂S abatement at the geysers power plant", *proceedings of the international symposium on Solving Corrosion and Scaling Problems in Geothermal Systems*, January 17-20, 1983, San Francisco, California (1983).
- Crabtree M., Eslinger D., Fletcher P., Miller M., Johnson A., King G., "Fighting Scale - Removal and Prevention", *Oilfield Review*, **Autumn**, 30-45 (1999).
- Emmons D.H., Graham G.C., Holt S.P., Jordan M.M. and Lorcardel B., "On-Site, Near-Real-Time Monitoring of Scale Deposition", *paper SPE 56776 presented at the SPE Annual Technical Conference and Exhibition*, Huston, Texas (1999).
- Gunarathne G.P.P. and Keatch R.W., "Novel Techniques for Monitoring and Enhancing Dissolution of Mineral Deposits in Petroleum Pipelines", *paper SPE 30418 presented at the Offshore Europe Conference*, Aberdeen UK (1995).
- Kevin K., "Operating Experiences for the World's First Commercially Installed Multiphase Meters in the Liverpool Bay Field", *paper presented at the IBC Conference on Multiphase Flow Metering*, London (1999).
- Moar P.N. *et al.*, "Fabrication, modelling and direct evanescent measurement of tapered optical fiber sensors", *Journal of Applied Physics*, 3395 (1999).
- Morizot A.P. and Neville A., "A Novel Approach for Monitoring of CaCO₃ and BaSO₄ Scale Formation", *paper SPE 60189 presented at the 2nd International Oilfield Scale Symposium*, Aberdeen, UK (2000).
- Poyet J-P., Ségéral G., Toskey E., "Real-Time Method for the Detection and Characterization of Scale", *paper SPE 74659 presented at the 4th International Oilfield Scale Symposium*, Aberdeen, UK (2002).
- Shleien B., "The Health Physics and Radiological Health Handbook", *revised edition*, Silver Spring Md. (1992).
- Smith J.K., Yuan M., Lopez T.H., Means M. and Przybylinski J.L., "Real-Time and *In-Situ* Detection of Calcium Carbonate Scale in a West Texas Oilfield", *paper SPE 80372 presented at the 5th International Oilfield Scale Symposium*, Aberdeen, UK (2002).
- Stamatakis E., Haugan A., Dugstad Ø., Muller J., Chatzichristos C., Bjørnstad T., Palyvos I., "Validation of Radiotracer Technology in Dynamic Scaling Experiments in Porous Media", *Chemical Engineering Science*, **60/5**, 1363-1370 (2005a).
- Stamatakis E., Stubos A., Palyvos I., Chatzichristos C., Muller J., "An improved predictive correlation for the induction time of CaCO₃ scale formation during flow in porous media ", has been accepted for publication in the *Journal of Colloid and Interface Science*, (2005b).

Söhnel O. and Mullin J.W., 1982. Precipitation of Calcium Carbonate. *Journal of Crystal Growth*, **60**: 239-250.

Theuveny B., Ségéral G. and Moksnes P.O., "Detection and Identification of Scales Using Dual Energy / Venturi Subsea or Topside Multiphase Flow Meters", *paper OTC 13152 presented at the Offshore Technology Conference*, Houston, Texas (2001).

8.1 Web site references

Soiltz-sous-Forêts project: www.soultz.net

MultiScale, Petrotech ASA: <http://www.petronett.com/multiscale/>

Appendix 1 – Result file from a single point calculation at 1 bar, 160°C

INPUT DATA

Water analysis no: geothermal brine GPK2 –S2.

ION	CONCENTRATION	
	mmol/l	mg/l
Na+ :	1225.47	28173.56
K+ :	73.66	2880.11
Mg2+ :	3.09	75.12
Ca2+ :	165.92	6650.07
Sr2+ :	0.00	0.00
Ba2+ :	0.00	0.00
Fe2+ :	1.74	97.18
Cl- :	1630.47	57800.16
Br- :	0.00	0.00
SO42- :	1.78	170.99
Total organic acid:	0.00 mmol/l	0.00 mg/l
Total alkalinity :	6.60 mmol/l	402.72 mg/l
Density will be determined by multiSCALE		

Fixed gas composition model. No mass balance data given

CALCULATION PARAMETERS

Fixed gas composition:

CO2 : 14.20 mole%
H2S : 0.00 mole%
CH4 : 85.80 mole%
C2 : 0.00 mole%
C5 : 0.00 mole%
C10 : 0.00 mole%

SINGLE POINT

Temperature: 160.00 C

Pressure : 1.00 bar

Water : geothermal brine

WATER COMPOSITION AND ACTIVITY COEFFISIENTS

Specie	Molality	Act. Coef.	Specie	Molality	Act. Coef.
H+	1.567899E-06	0.916432	OH-	5.904884E-06	0.313645
Na+	1.225470E+00	0.483579	Cl-	1.630470E+00	0.580227
K+	7.366000E-02	0.350996	Br-	0.000000E+00	0.531509
Mg2+	3.090000E-03	0.049719	SO42-	1.780000E-03	0.010372
Ca2+	1.634910E-01	0.081074	HCO3-	5.723502E-04	0.193806
Sr2+	0.000000E+00	0.037150	CO32-	5.759072E-07	0.004706
Ba2+	0.000000E+00	0.032956	HS-	0.000000E+00	0.281180
Fe2+	7.475393E-04	0.035929	Ac-	0.000000E+00	0.479835
HAc	0.000000E+00	1.000000			
CO2	1.087297E-03	1.088164			
H2S	0.000000E+00	0.999976			
CH4	6.418105E-04	1.560743			
CaCO3*	8.601555E-06	0.125355			
CaHCO3	8.206756E-04	0.193806			

*) Aqueous CaCO3, not solid

GENERAL INFO

Property	Initial	Equilibrium
pH :	6.4963	5.8426
Water activity:	0.9611	0.9611
Total CO2(aq) :	7.4769	2.4895 mmol/kg H2O
Total H2S(aq) :	0.0000	0.0000 mmol/kg H2O
Total CH4(aq) :	0.6417	0.6418 mmol/kg H2O
Alkalinity :	6.6000	1.4157 mmol/kg H2O
Ionic strength:	1.8054	1.8037 mol/kg H2O
Charge balance:	0.0000	0.0000 mmol/kg H2O
TDS :	96295.7018	95871.4871 mg/kg H2O

SATURATION RATIOS AND PRECIPITATED AMOUNTS

Salt	Initial SR	Precipitate g/M3	Equilibrium SR	Solubility product
FeS	0.000	0.0	0.000	2.2566E-02
FeCO3	47.163	115.0	0.999	4.3079E-10
CaCO3	20.016	160.1	1.000	9.4126E-08
CaSO4A	0.428	0.0	0.434	6.7055E-04
CaSO4G	0.038	0.0	0.039	7.5062E-03
BaSO4	0.000	0.0	0.000	4.2365E-07
SrSO4	0.000	0.0	0.000	7.3424E-05
NaCl	0.022	0.0	0.022	9.1453E+01

MASS BALANCES (%)

FIXED GAS COMPOSITION MODEL

COMPOSITION OF OIL/GAS PHASE (mole fractions)

COMP	OIL mole frac	GAS mole frac	Equil. K fug. coeff Gas/Oil
CO2	NO OIL	0.142000	0.999166 1.000000
H2S	NO OIL	0.000000	0.998509 1.000000
CH4	NO OIL	0.858000	0.999913 1.000000
C2	NO OIL	0.000000	0.998663 1.000000
C5	NO OIL	0.000000	0.995923 1.000000
C10	NO OIL	0.000000	0.991818 1.000000
C16	NO OIL	0.000000	0.987399 1.000000
C20	NO OIL	0.000000	0.984690 1.000000
C32	NO OIL	0.000000	0.976547 1.000000
C44	NO OIL	0.000000	0.967902 1.000000
H2O	NO OIL	0.000000	0.998930 1.000000
TOT	0.000000	1.000000	

EQUILIBRIUM CONSTANTS

Reaction	Thermodynamic	Stoichiometric
KH(CO ₂)	: 8.3391E-03	7.6570E-03
K1(CO ₂)	: 1.4016E-07	8.2534E-07
K2(CO ₂)	: 3.5104E-11	1.5776E-09
K(CaHCO ₃ ⁺)	: 1.0818E+02	8.7703E+00
K(CaCO ₃ (aq))	: 3.0017E+04	9.1355E+01
KH(H ₂ S)	: 2.8464E-02	2.8422E-02
K1(H ₂ S)	: 2.8612E-07	1.1103E-06
KH(CH ₄)	: 1.1676E-03	7.4803E-04
K(HAc)	: 5.5112E-06	1.2533E-05
K(water)	: 2.7688E-12	9.2583E-12

ERRORS. ALL NUMBERS SHOULD BE SMALL.

NB! Only errors for equilibra used in the calculation are printed

EQUILIBRIA

0 -0.64631E-01 %
 1 0.31428E-01 %
 6 0.00000E+00 %
 7 0.00000E+00 %
 8 0.00000E+00 %
 9 -0.11102E-13 %
 11 0.00000E+00 %
 12 0.00000E+00 %
 14 0.00000E+00 %

ERROR IN ION CONCENTRATIONS mol/kg H₂O

Fe²⁺: 0.00000E+00
 Ca²⁺: -0.18296E-17
 Na⁺: 0.00000E+00
 Cl⁻: 0.00000E+00
 SO₄²⁻: 0.00000E+00